

# Computational Modeling of Human Head Electromagnetics for Source Localization of Milliscale Brain Dynamics

Allen D. MALONY<sup>a,1</sup>, Adnan SALMAN<sup>b</sup>, Sergei TUROVETS<sup>c</sup>, Don TUCKER<sup>c</sup>,  
Vasily VOLKOV<sup>d</sup>, Kai LI<sup>c</sup>, Jung Eun SONG<sup>c</sup>, Scott BIERSDORFF<sup>b</sup>, Colin DAVEY<sup>c</sup>,  
Chris HOGE<sup>b</sup>, and David HAMMOND<sup>b</sup>

<sup>a</sup>*Dept. Computer and Information Science, University of Oregon*

<sup>b</sup>*Neuroinformatics Center, University of Oregon*

<sup>c</sup>*Electrical Geodesics, Incorporated*

<sup>d</sup>*Dept. Mathematics and Mechanics, Belarusian State University*

**Abstract.** Understanding the milliscale (temporal and spatial) dynamics of the human brain activity requires high-resolution modeling of head electromagnetics and source localization of EEG data. We have developed an automated environment to construct individualized computational head models from image segmentation and to estimate conductivity parameters using electrical impedance tomography methods. Algorithms incorporating tissue inhomogeneity and impedance anisotropy in electromagnetics forward simulations have been developed and parallelized. The paper reports on the application of the environment in the processing of realistic head models, including conductivity inverse estimation and lead field generation for use in EEG source analysis.

**Keywords.** Electromagnetics, head modeling, brain dynamics, EEG, localization.

## Introduction

Advances in human brain science have been closely linked with new developments in neuroimaging technology. Indeed, the integration of psychological behavior with neural evidence in cognitive neuroscience research has led to fundamental insights of how the brain functions and manifests our physical and mental reality. However, in any empirical science, it is the resolution and precision of measurement instruments that inexorably define the leading edge of scientific discovery. Human neuroscience is no exception. Brain activity takes place at millisecond temporal and millimeter spatial scales through the reentrant, bidirectional interactions of functional neural networks distributed throughout the cortex and interconnected by a complex network of white matter fibers. Unfortunately, current non-invasive neuroimaging instruments are unable to observe dynamic brain operation at these milliscales. Electromagnetic measures (electroencephalography (EEG), magnetoencephalography (MEG)) provide high temporal resolution ( $\leq 1$  msec), but their spatial resolution lacks localization of neural source activity. Hemodynamic measures (functional magnetic resonance

---

<sup>1</sup> Corresponding Author.

imaging (fMRI), positron emission tomography (PET)) have good 3D spatial resolution  $1\text{mm}^3$ , but poor temporal resolution on the order of seconds.

Our research goal for the last six years has been to create an *anatomically-constrained spatiotemporally-optimized neuroimaging (ACSON)* methodology to improve the source localization of dense-array EEG (dEEG). Anatomical constraints include high-resolution three-dimensional segmentation of an individual's head tissues, identification of head tissue conductivities, alignment of source generator dipoles with the individual's cortical surface, and interconnection of cortical regions through the white matter tracts. Using these constraints, the ACSON technology constructs a full-physics computational model of an individual's head electromagnetics and uses this model to map measured EEG scalp potentials to their cortical sources.

## 1. Methods

Modern dense-array EEG (dEEG) technology, such as the Geodesic Sensor Net [19] from Electrical Geodesics, Inc. (EGI) shown in Figure 1(left), can measure micro-volt potentials on the human scalp at up to 256 sensors every 1 msec or less. EEG signals are the consequence of current dipoles associated with postsynaptic activities of neuronal cells. A single postsynaptic potential produces a current-dipole moment on the order of 20 fAm (femtoampere  $\times$  meter) [9]. A  $10\text{mm}^2$  patch of the cortex surface contains approximately 100,000 neurons with thousands of synapses per neuron. At least 10 nAm is required to detect extracellular fields, and measurable EEG signals with a good signal-to-noise ratio require tens of millions of simultaneously activated synapses.

As seen in Figure 1 (right), cortical neurons are arranged parallel to each other and point perpendicular to the cortical surface. It is this structural arrangement that allows currents from groups of thousands of neurons to accumulate and generate an *equivalent current dipole* for a cortex surface region. Therefore, scalp potentials measured by dEEG can be modeled by the combined electrical potentials (called *lead fields*) produced by up to 10,000 or more cortex patches. That is the good news. The bad news is that the scalp potentials are a linear superposition of all the *distributed source* lead fields and the individual EEG contributors (i.e., the distributed source dipoles) must be disentangled to determine the dynamics of each brain region.

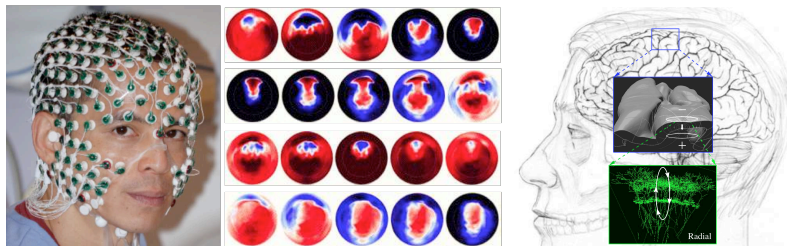


**Figure 1.** (Left) EGI 256-channel Geodesic Sensor Net for dEEG recording and topographical potential maps showing epileptic spike wave progression between 110-310 msec with 10 msec samples. (Right) Neuronal current flows perpendicular to the cortex and creates dipole fields. Because of cortex folding, these fields can be radial, tangential, and oblique in orientation.

*Localization Model.* The general distributed source localization problem can be stated as follows:  $\Phi = KS + E$ , where  $\Phi = [\varphi_1, \dots, \varphi_{N_e}]$  are  $N_e$  measured EEG signals over

$N_t$  time ( $N_e \times N_t$ ),  $K$  is the lead field matrix (LFM) linking  $N_s$  current sources to their electrical potential ( $N_e \times N_s$ ),  $S = [s_1, \dots, s_{N_s}]$  are the current source values over time ( $N_s \times N_t$ ), and  $E$  is error over time. Since the only variables are the source dipole magnitudes  $S$ , their solution is a classic linear inverse problem obtained by inverting  $\Phi$ . Unfortunately,  $N_s \gg N_e$ , making the problem ill-posed. Methods for solving the underdetermined distributed source inverse problem apply minimum norm estimates and their generalization with various regularization schemes to overcome the ill-posed nature of the problem [8,13,14]. No matter how sophisticated the inverse technique, they all depend on determining the forward projection of current dipoles with unit magnitudes to scalp electrical potentials at known sensor locations (i.e., the lead field matrix  $K$ ). Building  $K$  requires a model of the head electromagnetics.

*Electromagnetics Model.* Given a volume conductor  $\Omega$  with an arbitrary shape and  $\Gamma_\Omega$  as its boundary, a current density within the volume induces electric and magnetic fields  $E$  and  $B$  that can be measured on the conductor surface. If the conductivities  $\sigma$  and the electrical current sources  $S$  are known, the electric and magnetic fields inside the volume are fully described by Maxwell's equations. Thus, the electrical forward problem for the human head can be stated as follows: given the positions and magnitudes of neuronal current sources (modeled as distributed dipoles), as well as geometry and electrical conductivity of the head volume  $\Omega$ , calculate the distribution of the electrical potential on the surface of the head (scalp)  $\Gamma_\Omega$ . Mathematically, it means solving the linear Poisson equation:  $\nabla \cdot \sigma(x, y, z) \nabla \phi(x, y, z) = S$  in  $\Omega$  with no-flux Neumann boundary conditions on the scalp:  $\sigma(\nabla \phi) \cdot n = 0$ . Here  $n$  is the normal to  $\Gamma_\Omega$ ,  $\sigma = \sigma_{ij}(x, y, z)$  is an inhomogeneous tensor of the head tissues conductivity and  $S$  is the source current; if the head tissues are considered to be isotropic,  $\sigma$  is a scalar function of  $(x, y, z)$ , and — when they are orthotropic,  $\sigma$  is a diagonal tensor with off-diagonal — components  $\sigma_{ij} = 0, i \neq j$ .

*Conductivity Inverse Model.* If the head tissue conductivities are not known, it is necessary to solve the conductivity inverse problem by applying a general tomographic structure with a known current source, in this case current injected into the head at the scalp surface (this substitutes for neuronal current sources). From an assumed set of the average head tissue conductivities,  $\sigma_{ij}$ , and given an injection current configuration,  $S$ , it is possible to predict the set of potential measurement values,  $\phi^p$ , given a forward model,  $F$ , of head electromagnetics as the nonlinear functional by solving the Poisson equation above:  $\phi^p = F(\sigma_{ij}(x, y, z))$ . Once an appropriate objective function describing the difference between the measured scalp potentials,  $V$ , and the predicted potentials (at the sensor locations),  $\phi^p$ , is defined (e.g., least square norm), and a search for the global minimum is undertaken using advanced nonlinear optimization algorithms [10,15].

When head tissue conductivities are determined, the forward model can be used to create the *lead field matrix*  $K$  by individually activating each current dipoles with unit magnitude and calculating the scalp electrical potentials at the sensor locations. With the LFM formed, it is then possible to solve for the spatiotemporal source dipole magnitudes  $S$  given a dEEG waveform.

## 2. ACSON Design

The most critical component for source localization of dEEG measurements is the computational modeling of the electromagnetics of each subject. To build an

electromagnetics head model of the highest quality for an individual requires accurate anatomical constraints and biophysical parameters:

*High-resolution segmentation of head tissues.* Various imaging methods (e.g., magnetic resonance imaging (MRI) and computerized axial tomography (CAT)) can provide volumetric data of the human head. Since the biophysical properties of each tissue are different and we want to employ quantitative (as opposed to qualitative pixel-to-pixel) piece-wise constant tomographic reconstruction, image segmentation is necessary for modeling. The physical geometry of the segmented tissues forms the basis for the 3D computational model.

*Determination of tissue conductivities.* The human head tissues are inhomogeneous (different tissues have different conductivities) and anisotropic (conductivity can change with respect to orientation and other factors). None of the internal head tissues can be measured directly and noninvasively. They must be determined through bounded electrical impedance tomography (bEIT) and inverse modeling [4,15,16,17,20,21,22].

*Cortex surface extraction and tessellation.* To build a lead field matrix, dipole generators must be placed at locations normal to the cortex surface. Cortex tessellation creates regions for dipole placement.

Our research has produced methods and technologies to address these requirements. The ACSO environment shown in Figure 2 integrates the tools in a processing workflow that inputs head imagery (MRI, CT), bEIT data, and EEG sensor registration information and generates automatically accurate LFM for use in source localization

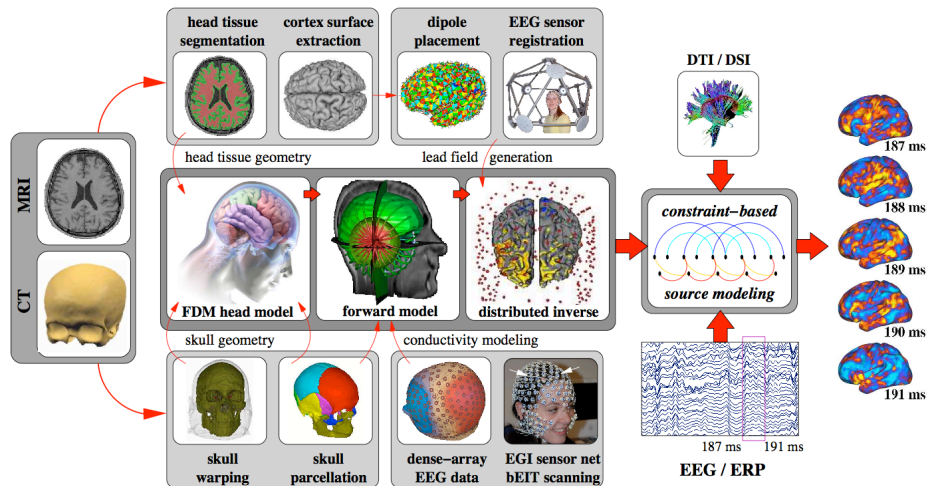


**Figure 2.** The ACSO framework supports a workflow of MRI/CT image processing and electromagnetics modeling to deliver a lead field matrix for a single individual to use in source localization. The brain images on the right portray scalp EEG source-mapped to cortex locations.

### 3. Results

The ACSO environment implements all the head modeling capabilities necessary for high-resolution source localization, but it has never been used until now to produce a

real head model and LFM for an individual that can be applied in source localization. We selected Dr. Colin Holmes (a.k.a. “colin27” in the Montreal Neurological Institute (MNI) BrainWeb database [2]) for this purpose. The MNI wanted to define a brain representative of the standard adult male population. They took 250 normal MRI scans, scaled landmarks to equivalent positions on the Talairach atlas [18], and averaged them with 55 additional registered images to create the “MNI305” dataset. In addition, one of the MNI lab members (Dr. Holmes) was scanned 27 times, and the scans were coregistered and averaged to create a very high detail MRI dataset of one brain. When compared to MNI305, it turned out that Dr. Holmes’ brain was (is) very close to the average head standard! While colin27 provides the necessary MRI data for segmentation, ACSON also requires bEIT scans. Luckily, Dr. Holmes has been a long-time collaborator with our group. Last year, he agreed to have 64 bEIT scans made.

### *3.1. Head Electromagnetics Forward Solver.*

The ADI and VAI forward solution methods for electromagnetic should first be validated with respect to a known solution. The source localization field has long used a concentric k-shell sphere model ( $k=3,4$ ) as a theoretical standard of reference (each shell represents a head tissue), since analytical solutions are known for the isotropic and anisotropic case [3,5]. We created a 4-sphere testcase with  $100 \times 100 \times 100$  voxels and achieved a near-perfect correspondence between the theoretical isotropic and ADI results for a set of shell conductivities. Analytical solutions for spherical anisotropic models [3] are also available for VAI validation. We achieved very good accuracy with respect to the spherical model in both cases, lending strong confirmation that the algorithm is working properly.

Based on these findings, the colin27 MRI dataset was segmented at  $(2\text{mm})^3$  and  $1\text{mm}^3$  resolutions into five tissue: scalp, skull, CSF, gray matter, and white matter. We built ADI and VAI head models and computed a forward solution for each resolution case for known conductivities and current sources. These models were evaluated relative to each other and then used for conductivity inverse and lead field calculations.

### *3.2. Conductivity Inverse Solution*

The ADI and VAI forward solvers for electromagnetic head modeling are the core computational components for the conductivity inverse and lead field matrix calculations. The conductivity inverse problem will need to process the bEIT measurements for up to 64 current injection pairs in the general case. Depending on the number of conductivity unknowns, each conductivity search for a single pair will require many thousands of forward solutions to be generated. Placement of current injection points is important to maximize the bEIT measurement value. Running the full complement of pairs enables the solution distribution to be better characterized.

For all of our experiments, we set the number of tissue conductivity parameters to three: scalp, skull, and brain. Using the  $1\text{mm}^3$  colin27 head model, a simulated annealing optimization process was applied to search for optimum values for all 64 EIT pairs. Histogram plots of conductivity solutions for all pairs were fitted with a normal distribution to determine mean and standard deviation. While other groups have reported research results for human head modeling and conductivity analysis (see [1,6,11,12]), our results are impressive because they are the first results in the field determined by dense array bEIT scanning, high-resolution subject-specific MRI/CT

based FDM of the human head, and simultaneous 3D search in the space of unknown conductivities. The derived brain/skull resistivity ratio is confirmed to be in the 1:20 to 1:30 range reported by other research groups [7,23].

### *3.3. Lead Field Matrix Generation*

Once tissue conductivity estimates are determined, they can be used to calculate the lead field for all current dipoles of interest. Because the ACSO methodology is based in finite difference modeling, it is necessary to represent the dipoles normal to the cortex surface as vector triplets in x, y, z whose weighted combination determines the normal vector. The consequence is that three forward solves must be run, one for each axis orientation, for every dipole in three-space. We created an isotropic LFM and an anisotropic LFM for colin27 based on 4,836 axis dipoles. This required 9,672 forward solutions to be computed (half for ADI, half for VAI) by activating only one dipole and calculating the scalp projection. For each projection, we capture the value for 1,925 potential sensor locations. Thus, each LFM is 4836 x 1925 in size.

### *3.4. Source Localization*

Our efforts at building the most accurate electromagnetics head model culminate in the use of the LFM for source localization. We created an anisotropic LFM from a 1mm<sup>3</sup> head model for 979 dipoles at 8mm spacing (2937 axis dipoles). For each dipole, we chose the LFM column representing that dipole's scalp EEG projection at 1925 potential sensors locations and input the values for source localization. Magnitudes for all the dipoles were computed using sLORETA [14] and the one with the maximum intensity was determined and the 3D distance from the "true" dipole measured. Even with a noise level of 10%, the maximum magnitude dipole source localized with a anisotropic LFM is within 6.37mm of a 8mm spaced target dipole. The isotropic LFM is significantly worse. The bottom line is that modeling anisotropy in human head electromagnetics simulation is important for improving the accuracy of linear inverse distributed source solutions.

## **4. Conclusion**

We have created the ACSO methodology and environment to address one of the most challenging problems in human neuroimaging today – observing the high-resolution spatiotemporal dynamics of a person's brain activity noninvasively. If such a capability existed, it would significantly advance neurological research and clinical applications, providing a powerful tool to study neural mechanisms of sensory/motor and cognitive function and plasticity, as well as improving neuromonitoring and neurorehabilitation for epilepsy, stroke, and traumatic brain injury. Our work provides an initial demonstration of the utility of full-physics modeling of human head electromagnetics and accurate head tissue conductivity assessment in improving the accuracy of electrical source localization. The ACSO modeling methods have been validated with analytical solutions and experimental results confirming prior research findings in the field.

**Acknowledgment.** This work was supported by a contract from the Department of Defense, Telemedicine Advanced Technology Research Center (TATRC).

## References

- [1] M.Clerc, G.Adde, J.Kybic, T.Papadopoulo, J.-M.Badier, In vivo conductivity estimation with symmetric boundary elements, *International Conference on Bioelectromagnetism*, May 2005.
- [2] C. Cocosco, V. Kollokian, R. Kwan, G. Pike, A. Evans, Brainweb: Online interface to a 3D MRI simulated brain database, *NeuroImage*, **5**:425, 1997.
- [3] J. de Munck, T. Faes, A. Hermans, R. Heethaar, A parametric method to resolve the ill-posed nature of the EIT reconstruction problem: a simulation study, *Annals of the New York Academy of Sciences*, **873**:440–453, 1999.
- [4] B. Esler, T. Lyons, S. Turovets, D. Tucker, Instrumentation for low frequency studies of the human head and its validation in phantom experiments, *International Conference on Electrical Bioimpedance*, April 2010.
- [5] T. Ferree, J. Eriksen, D. Tucker, Regional head tissue conductivity estimation for improved EEG analysis, *IEEE Transactions on Biomedical Engineering*, **47**(12):1584–1592, 2000.
- [6] S.Goncalves, et al., The application of electrical impedance tomography to reduce systematic errors in the EEG inverse problem: a simulation study, *Physiological Measurement*, **21**(3):379–393, 2000.
- [7] S. Goncalves, et al., In vivo measurement of the brain and skull resistivities using an EIT-based method and realistic models for the head, *IEEE Transactions on Biomedical Engineering*, **50**(6):754–767, June 2003.
- [8] R. Greenblatt, A. Ossadtchi, M. Pieger, Local linear estimators for the bioelectromagnetic inverse problem, *IEEE Transactions on Signal Processing*, **53**(9):3403–3412, Sept. 2005.
- [9] M. Hamalainen, J. Sarvas, Realistic conductivity geometry model of the human head for interpretation of neuromagnetic data, *IEEE Transactions on Biomedical Engineering*, **36**:165–171, Feb 1989.
- [10] S. Kirkpatrick, C. Gelatt, M. Vecchi, Optimization by simulated annealing, *Science*, **4598**:671–680, May 1983.
- [11] J. Meijs, O. Weier, M. Peters, A. van Oosterom, On the numerical accuracy of the boundary element method, *IEEE Transactions on Biomedical Engineering*, **36**:1038–1049, 1989.
- [12] T. Oostendorp, J. Delbeke, D. Stegeman, The conductivity of the human skull: results of in vivo and in vitro measurements, *IEEE Transactions on Biomedical Engineering*, **47**(11):1487–1492, 2000.
- [13] R. Pascual-Marqui, Review of methods for solving the EEG inverse problem, *International Journal of Bioelectromagnetism*, **1**(1):75–86, 1999.
- [14] R. Pascual-Marqui, Standardized low resolution brain electromagnetic tomography (sloreta): Technical details, *Methods and Findings in Experimental and Clinical Pharmacology*, **24**(5):22612, 2002.
- [15] A. Salman, A. Malony, S. Turovets, D. Tucker, Use of parallel simulated annealing for computational modeling of human head conductivity, In Y.S. et al., editor, *International Conference on Computational Science*, LNCS **4487**:86–93. Springer-Verlag, 2007.
- [16] A. Salman, S.Turovets, A.Malony, Computational modeling of human head conductivity, In V. S. et al., editor, *International Conference on Computational Science*, LNCS **3514**:631–638, Springer-Verlag, May 2005.
- [17] A. Salman, et al., Noninvasive conductivity extraction for high-resolution EEG source localization, *Advances in Clinical Neuroscience and Rehabilitation*, **6**:27–28, 2006.
- [18] J. Talairach and P. Tournoux., Co-planar stereotaxic atlas of the human brain, *Thieme*, Stuttgart, 1988.
- [19] D.Tucker, Spatial sampling of head electrical fields: the geodesic sensor net, *Electroencephalography and Clinical Neurophysiology*, **87**(3):154–163, 1993.
- [20] S. Turovets, et al., Bounded electrical impedance tomography for non-invasive conductivity estimation of the human head tissues, *Electrical Impedance Tomography Conference*, June 2009.
- [21] S. Turovets, et al., Conductivity analysis for high-resolution EEG, *International Conference on BioMedical Engineering and Informatics*, **2**:386–393, 2008.
- [22] V. Volkov, A. Zherdetsky, S. Turovets, A. Malony, A fast BICG solver for the isotropic poisson equation in the forward EIT problem in cylinder phantoms, *International Conference on Electrical Bioimpedance*, Gainesville, FL, April 2010.
- [23] Y. Zhang, W. van Drongelen, B. He, Estimation of in vivo brain-to-skull conductivity ratio in humans, *Applied Physics Letters*, **89**:2239031–3, 2006.